Earth and Planetary Science Letters 496 (2018) 248–256

Contents lists available at ScienceDirect

Earth and Planetary Science Letters

www.elsevier.com/locate/epsl

A 43 kyr record of protist communities and their response to oxygen minimum zone variability in the Northeastern Arabian Sea

Kuldeep D. More [a,b,*], William D. Orsi [c,d], Valier Galy [e], Liviu Giosan [f], Lijun He [g], Kliti Grice [b], Marco J.L. Coolen [b,*]

[a] Department of Agriculture and Environment, School of Molecular and Life Sciences (MLS), Curtin University, Bentley, WA 6102, Australia
[b] Western Australia Organic and Isotope Geochemistry Centre (WAOIGC), The Institute for Geoscience Research (TIGeR), School of Earth and Planetary Sciences (EPS), Curtin University, Bentley, WA 6102, Australia
[c] Department of Earth and Environmental Sciences, Paleontology & Geobiology, Ludwig-Maximilians-Universität München, 80333 Munich, Germany
[d] GeoBio-Center LMU, Ludwig-Maximilians-Universität München, 80333 Munich, Germany
[e] Department of Marine Chemistry and Geochemistry, Woods Hole Oceanographic Institution, Woods Hole, MA 02543, USA
[f] Department of Geology and Geophysics, Woods Hole Oceanographic Institution, Woods Hole, MA 02543, USA
[g] State Key Laboratory of Estuarine and Coastal Research, East China Normal University, Shanghai, 200062, China

ARTICLE INFO

Article history:
Received 6 December 2017
Received in revised form 23 May 2018
Accepted 25 May 2018
Available online 18 June 2018
Editor: D. Vance

Keywords:
Northeast Arabian Sea
oxygen minimum zone
protist ecology
sedimentary ancient DNA
paleogenomics
glacial–interglacial cycle

ABSTRACT

An extensive oxygen minimum zone (OMZ) occurs in the northeastern (NE) Arabian Sea where sedimentary records show evidence of alternating strong and weak OMZs that correlate with North Atlantic climate variability during the last glacial–interglacial cycle. OMZs are expanding world-wide, but information on long-term OMZ-ecosystem interactions is mainly limited to fossilized species, notably foraminifera. Here, we provide a first comprehensive ancient sedimentary DNA record of both fossilizing and non-fossilizing protists and their response to OMZ variability in the NE Arabian Sea over the last 43 ka. Protist communities changed significantly during strong vs. weak OMZ conditions coincident with interstadials and stadials respectively. Dinoflagellates were identified as significant indicator taxa for strong OMZs during glacial as well as interglacial interstadials, whereas diatoms were significant indicators for strong OMZs only during glacial interstadials. The chlorophyte *Chlorella* was found to be the main phototrophic protist in nutrient-depleted surface waters during glacial stadials. Notably, strong OMZ conditions shaped past protist communities by creating isolated habitats for those capable of sustaining oxygen depletion either by adapting a parasitic life cycle (e.g. apicomplexans) or by establishing mutualistic connections with others (e.g. radiolarians and mixotrophic dinoflagellates) or by forming cysts (e.g. colpodeans). Notably, a long-term increase in eutrophication and a decrease in the diatom/dinoflagellate ratio was observed during the late Holocene favoring the pelagic component of the marine food web. A similar scenario could be expected in the context of predicted worldwide expansion of coastal OMZs associated with global climate change.

© 2018 Elsevier B.V. All rights reserved.

1. Introduction

1.1. Oxygen minimum zone (OMZ)

Over geological timescales, recurring changes in the ocean oxygenation have resulted in multiple biotic crises with concomitant changes in marine ecosystems and climate balance (Wright et al., 2012). Over the last few decades, decline in oxygen concentrations has been observed throughout much of the world ocean's interior and is predicted to continue in the context of coastal eutrophication and global warming (Helm et al., 2011; Keeling et al., 2010). Upwelling of nutrients promote the formation of plankton blooms. Oxygen consumption through bacterial degradation of this sinking biomass and thermal stratification of the water column contribute to a decreased oxygen availability leading to the formation and expansion of oxygen minimum zones (OMZs) at mid water depths (~150–1300 m) (Schulz et al., 2002). Selective pressure under OMZ conditions has been observed in unicellular eukaryotes (protists), which are major components of the oceanic food chain and are important contributors to and consumers of pelagic productivity (Burkill et al., 1993; Strom and Welschmeyer, 1991; Worden et al., 2015). Photosyn-

* Corresponding authors.
E-mail addresses: k.more@postgrad.curtin.edu.au (K.D. More), marco.coolen@curtin.edu.au (M.J.L. Coolen).

https://doi.org/10.1016/j.epsl.2018.05.045
0012-821X/© 2018 Elsevier B.V. All rights reserved.

thetic protists are major primary producers inhabiting the photic zone, while bacterivorous and planktivorous heterotrophs bridge the prokaryotic component of the food web to higher trophic levels and follow the distribution of autotrophic protists. Mixotrophs being capable of autotrophy and phagotrophy, have a much wider distribution across the water column (Sherr and Sherr, 1994) and can be directly exposed to oxygen stress at intermediate depth (Jing et al., 2015). Shoaling of the upper boundaries of the OMZs can affect protist habitats and *vice versa*, changes in the distribution of primary producers and consumers can affect the oxygen demand and, hence the distribution of OMZs.

1.2. Modern observations: OMZ vs protists

The northeastern Arabian Sea experiences semi-annual monsoonal wind reversals contributing to two periods of heightened surface productivity: during the southwest (SW) monsoon (June–September) and during the northeast (NE) monsoon (November–February) (Parab et al., 2006). Strong SW monsoonal winds lead to north-eastward drift of nutrient-rich surface waters from Oman to the Pakistan margin causing high primary productivity (Andruleit et al., 2000; Schulte and Muller, 2001; Schulz et al., 2002). While during NE monsoon sea surface cooling activates the convection processes causing deep mixing of subsurface waters. This process leads to injection of nutrients to surface waters bolstering high winter pelagic productivity (Madhupratap et al., 1996). Microscopic cell counts and pigment analysis revealed that during the SW monsoon when nitrate concentrations are high, diatoms become dominant along with prymnesiophytes (Parab et al., 2006). By the end of the SW monsoon, sinking biomass of decaying diatom blooms provides substrate for microbial degradation, which causes rapid oxygen consumption at intermediate depth and intensification of the OMZ (Parab et al., 2006; Schulz et al., 2002). During this period, nitrate concentrations become undetectable and a shift from diatoms and prymnesiophytes to dinoflagellates below the shallow pycnocline is observed (Parab et al., 2006). In the oxygenated surface waters, where nitrate is below detection limits, pico-cyanobacterial populations then become dominant (Parab et al., 2006). During the NE monsoon, low nitrate concentration causes the replacement of a mixed diatom-dinoflagellate population by the nitrogen-fixing cyanobacterium *Trichodesmium*. A combination of low phytoplankton biomass and high ammonium concentrations further suggest that active grazers prevent the establishment of diatom-dinoflagellate blooms in the eastern Arabian Sea during the NE Monsoon. In May, just prior to the start of the SW Monsoon, nutrient enrichment associated with the demise and decay of *Trichodesmium* blooms along with coastal upwelling of nitrates stimulate the growth of both diatoms and dinoflagellates (Parab et al., 2006).

Information on these OMZ-ecosystem interactions in the Arabian Sea and elsewhere is mainly based on such recent observations, modeling experiments, and fossilized foraminifera (Blackford and Burkill, 2002; Madhupratap et al., 1996; Parab et al., 2006; von Rad et al., 1999). A holistic overview of past OMZ-protist interactions is lacking world-wide since the majority of the above-mentioned protist taxa do not fossilize. However, even in the absence of microfossils, genetic signatures of past planktons were found to be preserved in the marine geological records and can be used to reconstruct marine ecosystem changes caused by environmental perturbations (Coolen et al., 2013; Inagaki et al., 2005; Lejzerowicz et al., 2013).

1.3. Coring location in northeastern (NE) Arabian Sea

Records close to the Indus Canyon show that during the last glacial–interglacial cycle the NE Arabian Sea witnessed alternate strong and weak OMZs (Banakar et al., 2010; von Rad et al., 1995; Schulz et al., 1996), which makes it an ideal location to study long-term protist-OMZ interactions. For this study, we used highly resolved profiling of sedimentary protist 18S ribosomal RNA genes at centennial-scale resolution to reconstruct the interplay between past OMZ variability and protist community structures over the last glacial–interglacial cycle in the NE-Arabian Sea. The core used for this study was obtained from the centre of the OMZ on the continental slope, NW of the Indus Canyon (Orsi et al., 2017). Geochemical analysis revealed a distinct pattern of laminated, organic carbon-rich intervals comparable to those present in previously studied cores, which were obtained in close vicinity and at comparable water depths within the OMZ (von Rad et al., 1995).

Here, integrated analysis of the sedimentary DNA and paleoceanographic proxy data revealed unprecedented details about long-term effects of OMZ conditions on protist communities. Similar approaches could potentially reveal insights about long-term OMZ-ecosystem interactions at important OMZ locations other than the Arabian Sea.

2. Methods

2.1. Sample collection and storage

For this study, a 13-m-long Piston core 11C spanning 43 kyr of deposition was obtained during R/V Pelagia cruise 64PE300 from the center of the OMZ (566 m depth) on the continental slope NW of the Indus Canyon (23°N; 66°E). Subsamples (214 two-cm-thick intervals) for DNA and geochemical analysis were taken aseptically inside the ancient DNA-dedicated clean lab at the Woods Hole Oceanographic Institution (WHOI) as described in detail recently (Orsi et al., 2017). In that study, the same intervals of this core have been used to reveal to what extent the sub-seafloor microbiome was shaped by past OMZ conditions (Orsi et al., 2017).

2.2. Age model

Radiocarbon dates were obtained for the Holocene interval from mixed planktonic foraminifera or monospecific *Orbulina universa* samples (Orsi et al., 2017). Calibration was performed using Calib 7.1 with a reservoir age of 565 ± 35 radiocarbon years (Stuiver and Reimer, 1993). For pre-Holocene sediments, the age model is based on correlative tie points from XRF-derived Br record in core 64PE300-11C to the high-resolution total organic carbon records of nearby core SO90-136KL (Schulz et al., 1998). Linear interpolation was used to determine ages for each individual sample.

2.3. Bulk geochemistry

The intact archived core sections were scanned for bulk elemental composition using an ITRAX™ micro-XRF scanner with a molybdenum x-ray tube with a step-size of 200 µm for an exposure time of 10 s^{-1}. Bromine variability was used as proxy for organic matter (Ziegler et al., 2008). Total organic carbon (TOC), $\delta^{13}C$, $\delta^{15}N$, and C/N were analyzed using a Delta Plus stable light isotope mass spectrometer from 214 freeze-dried and carbonate-free sediment samples spanning the entire core as described in detail elsewhere (Orsi et al., 2017).

2.4. Sedimentary DNA extraction and analysis

Inside the ancient DNA-dedicated lab at WHOI, genomic DNA was extracted and purified from 5–10 g of wet weight sediment after Direito et al. (2012) with modifications described for this core in detail recently (Orsi et al., 2017). This protocol was repeated without the addition of sediment and the resulting extract was used as a control for contamination during extraction

and purification of the sedimentary DNA. The recovered purified sedimentary DNA was quantified fluorometrically using Quant-iT PicoGreen™ double stranded DNA (dsDNA) Reagent (Invitrogen) and ~20 nanograms of each extract was used as template for PCR (Polymerase chain reaction) amplification of preserved planktonic 18S ribosomal RNA (rRNA) genes. The short ~130 base pair (bp)-long 18S rDNA-V9 region was amplified using the domain-specific primer combination 1380F (5′-CCC TGC CHT TTG TAC ACA C-3′) and 1510R (5′CCT TCY GCA GGT TCA CCT AC-3′) (Amaral-Zettler et al., 2009). Quantitative PCR (qPCR) was performed using a SYBR®Green I nucleic acid stain (Invitrogen) and using a Realplex qPCR system (Eppendorf, Hauppauge, NY). The annealing temperature was set to 66 °C and all reactions were stopped in the exponential phase after 35–42 cycles.

To generate template for subsequent Illumina MiSeq sequencing of PCR-amplified sedimentary 18S rRNA genes, the same qPCR conditions and region-specific primers were used, except for that the primers included the Illumina flowcell adapter sequences as well as the pad regions (Caporaso et al., 2012). The reverse primer now also included a unique 12 base Golay barcode sequence to support pooling of the samples. The quality of the PCR products was verified by agarose gel electrophoresis and equimolar amounts of the barcoded PCR products were pooled and purified using the AMPure®XP PCR purification kit (Agencourt Bioscience Corp., Beverly, MA). Four hundred nanograms of the mixed and purified barcoded amplicons were subjected to subsequent Illumina MiSeq sequencing using the facilities of the W.M. Keck Center for Comparative and Functional Genomics, University of Illinois at Urbana-Champaign, IL, USA. The sequenced 18S libraries resulted in approximately 12 million reads. QIIME was used for further processing of rRNA gene sequences (Caporaso et al., 2010). Reads were organized into Operational Taxonomic Units (OTUs) after passing quality control (95% sequence identity with UCLUST) and assigned to taxonomic groups through BLASTn searches against the SILVA database (Pruesse et al., 2007). OTU tables were rarified in QIIME using the single_rarefaction.py command to the sample and singletons as well as non-protist reads were removed. Ecological statistics were calculated in R (https://www.r-project.org) using a Bray Curtis distance in the Vegan package (Oksanen, 2011). Analysis of Similarity (ANOSIM) was carried out using 999 permutations with a Bray Curtis distance (Clarke, 1993). Indicator Species Analysis (ISA) (Dufrene and Legendre, 1997) was performed in the Vegan package and significance was tested with a nonparametric procedure involving the Monte-Carlo permutation procedure with 999 permutations.

3. Results

3.1. Chronology of the core and paleo-environment

The age model used to establish the timing of depositional and environmental changes is based on radiocarbon dating of foraminiferal carbonates and a comparison between XRF-derived bromine (Br) (Orsi et al., 2017) and TOC content (Fig. 1) to highly resolved TOC data from well-dated comparable core from the same location (Schulz et al., 1998). Bromine, a biophilic halogen that binds to allochthonous marine organic matter (Ziegler et al., 2008) and TOC values correlate significantly ($r = 0.65$, $P < 0.01$), which suggests a marine origin of the majority of organic matter over the last 43 Kyr. This is consistent with invariably low contributions of terrigenous OM from the Indus basin (Clift et al., 2010). Bulk sedimentary stable N isotope (δ^{15}N) compositions above ~6.5‰ are indicative of strong paleo-denitrification and strong OMZ conditions. Since TOC preservation was enhanced when OMZ conditions penetrated the coring location, variations in sedimentary TOC content during enhanced preservation likely reflect changes in paleo-productivity. The TOC content correlates positively with bulk δ^{15}N values ($r = 0.37$, $P < 0.01$) (Orsi et al., 2017). Based on δ^{15}N and TOC content we observed three depositional categories throughout the core: 1) Sapropelic sediments (TOC > 2 wt.%) with δ^{15}N values > 6.5‰ indicative of respectively high primary productivity and strong OMZ conditions; 2) Non-sapropelic sediments (TOC < 2 wt.%) and δ^{15}N values above 6.5‰ indicative of reduced primary productivity yet strong OMZ conditions; 3) Non-sapropelic sediments with δ^{15}N <6.5‰ representing weak or no OMZ conditions. Since the surface sediments were likely to be oxygenated during weak OMZ conditions, we cannot conclude whether reduced productivity or low preservation contributed to the lower TOC content in category 3 sediments.

During Oxygen Isotope stage (OIS) 2 and 3, the timing of deposition of Category 1 sapropelic sediments is coincident with North Atlantic millennial-scale Dansgaard–Oeschger (D/O) warm interstadials (Table S1). Category 1 sediments were also deposited during the Bølling/Allerød (BA) (~13–14.5 ka BP) and the Holocene (starting at ~10 Ka BP), when TOC content reached a maximum of 4 wt%. Category 2 sediments were mainly deposited during the transitions between stadials and interstadials, while Category 3 bioturbated sediments coincided with the timing of stadials, notably Heinrich (H) events and the Younger Dryas (YD) (~11.4–13 ka BP) (Table S1).

3.2. Past protist diversity

The sequenced eukaryotic library resulted in 2863 OTUs in 13 protist phyla: Alveolata, Amoebozoa, Apuszoa, Centroheliozoa, Chlorophyta, Choanoflagellida, Cryptophyta, Euglenozoa, Haptophyta, Jakobida, Rhizaria, Rhodophyta and Stramenopiles. Changes in the relative abundance of the most abundant phyla and their subgroups were compared with paleoenvironmental changes in the NE Arabian Sea during the last glacial interglacial cycle (Fig. 1 and Fig. 2).

Rhizaria is a supergroup of pelagic as well as benthic protists and comprise (a) Radiolaria, which are particle feeding or predatory zooplankton that can also form symbiotic relationships with e.g. dinoflagellates, (b) Cercozoa comprising various amoebae and flagellates, and (c) Foraminifera (Cavalier-Smith, 2002). In our dataset, Rhizaria represented 50–100% of the protistal reads in the majority of sediments deposited during strong OMZ conditions, notably during IS8, 7, 6, 3, 2, B/A, and the Holocene (Fig. 1). In contrast, a low relative abundance was observed especially during H1, H3, H4 and S11 (Fig. 1). Furthermore, a sharp decline in Rhizaria reads occurred between 8 to 8.5 kyrs, coinciding with the timing of the 8.2 ka cold event (Kobashi et al., 2007). The majority of Rhizaria belonged to the class Polycystinea (fossilizing radiolarians with silicate exoskeletons) (Fig. 2). Their relative abundance gradually increased over the course of the Holocene to reach 100% of Rhizaria reads (Fig. 2). Polycystines showed a sharp decline during H1 and H3. Polycystinea contains two major orders: Spumellaria and Nassellaria. Spumellarians were present during all climate stages (>25% of total Polycistinea reads) showing a general increasing trend after OIS2 (Fig. 3). Nassellarians were the most abundant Rhizaria during the LGM and H1 (Fig. 3). Cercozoa were relatively abundant (up to 50% of total rhizarian reads) during late H4, IS6, IS4 and H1 (Figs. 2 and 3).

Alveolata comprised up to 50 to 90% of total reads after the OIS3 to OIS2 transition (Fig. 1). This superphylum consist of protists with flattened vesicles known as alveoli and comprise dinoflagellates (Dinophyceae), ciliates (Ciliophora), and obligate parasites (Apicomplexa) (Cavalier-Smith, 1991) (Fig. 2). Dinoflagellate reads comprised more than 75% of the identified Alveolata during OIS2, except for a low relative abundance during H2 and YD-B/A transition. They were furthermore consistently abundant during

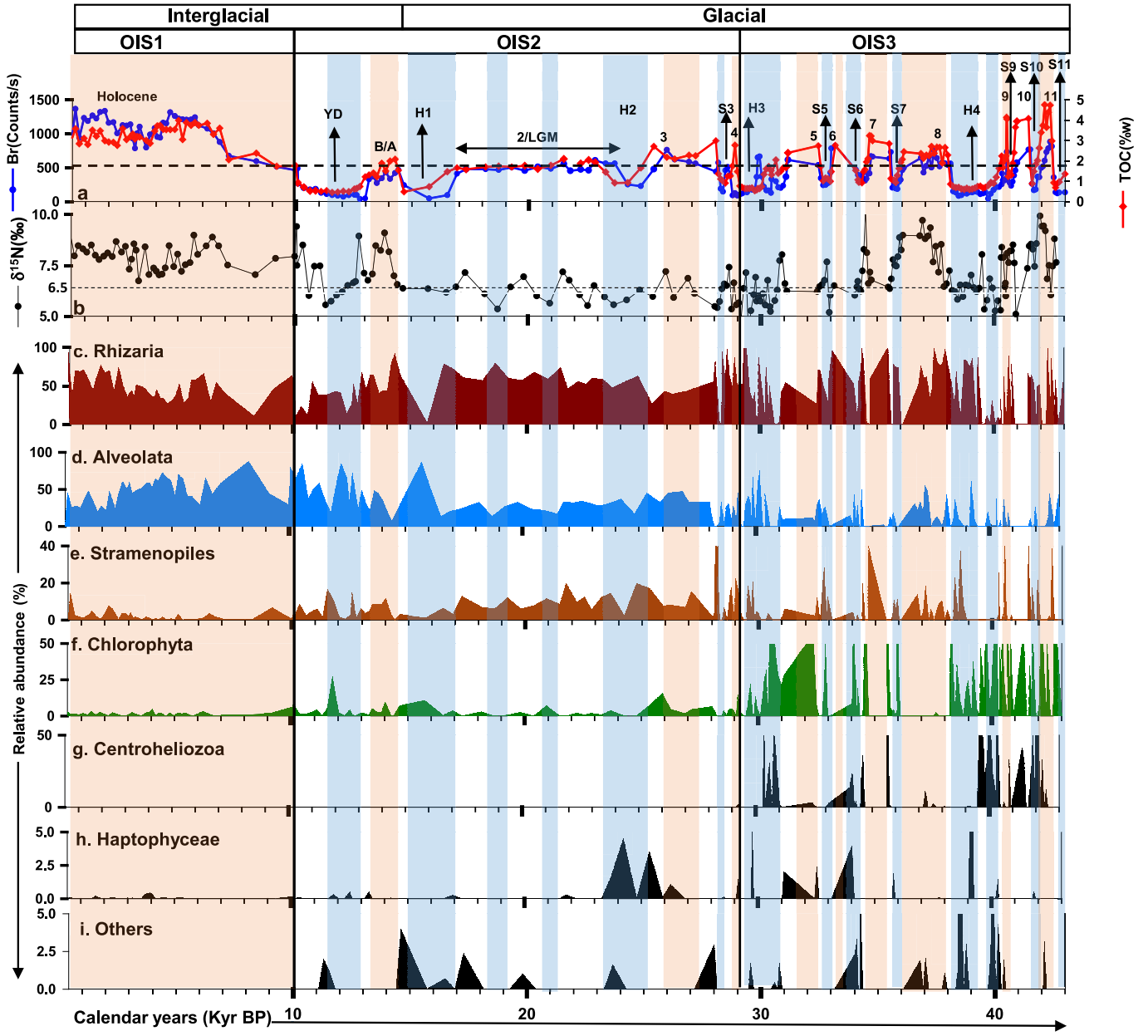

Fig. 1. Overview of protist group abundance throughout the core. (a) Bromine XRF profile (blue) correlated with TOC content (red). (b) δ^{15}N record. Values above 6.5 (dotted line) represent higher denitrification rates. (c)–(i) Relative abundance (%) of key protist groups. (i) Includes the sum of Amoebozoa, Apusozoa, Choanoflagellida, Rhodophyta, Euglenozoa, Jakobida, Cryptophyta. Vertical black lines denote OIS transitions. Vertical dark pastel orange boxes indicate strong OMZ conditions with high paleoproductivity, uncolored region indicates strong OMZ conditions with low paleoproductivity and pastel blue boxes indicate weak OMZ conditions. Interstadials are numbered on top of the TOC peaks while stadials are shown by arrows. Abbreviations: OIS (Oxygen Isotope Stage), YD (Younger Dryas), B/A (Bølling–Allerød), H (Heinrich event), IS (Interstadial), S (Stadial).

the Holocene, with the exception of a short decline at ~3.5 Ka BP (Fig. 2). The dinoflagellates identified in our core belonged to four major orders: (1) Blastodiniales, known parasites of zooplanktons (Coats, 1999), represented 25–65% of dinoflagellate reads during most of OIS2 (Fig. 3). (2) Mixotrophic Gymnodiniales, which lack an armored exterior, were mostly present during interstadials of OIS3 where they represented 90–100% of dinoflagellate reads. (3) Syndiniales, known endosymbionts or parasites of other dinoflagellates and zooplankton (Coats, 1999), were also found mainly during OIS3 (Fig. 3). (4) The less well-described Lophodiniales were mostly present during stadials S7, S6 (OIS3) and S3, H2 (OIS2).

A scattered predominance of ciliate reads was observed during OIS3 while they were consistently abundant alveolates during the B/A and YD (Fig. 2). They were dominated by the class Colpodea and Oligohymenophorea (Fig. 3). Colpodea, which are mainly freshwater ciliates, represented 80–95% of ciliate reads from H1 to Early Holocene. Oligohymenophorea (mostly microphagous ciliates) were the most abundant ciliate reads in interstadials like IS8, IS5, IS4, IS2 and Holocene with notable exception of the S6 stadial where they represented 90% of the ciliate reads (Fig. 3). Apicomplexa were sporadically present throughout the record (Fig. 2). More specifically, according to the detailed averaged dataset, reads related to the fish parasites Coccidia predominated the Apicomplexan reads during OIS2 and OIS1 (Fig. 3).

Unicellular Stramenopiles, consisting mainly of photosynthetic diatoms in our record, were relatively abundant protists mainly during interstadials in OIS3. They were most consistently present

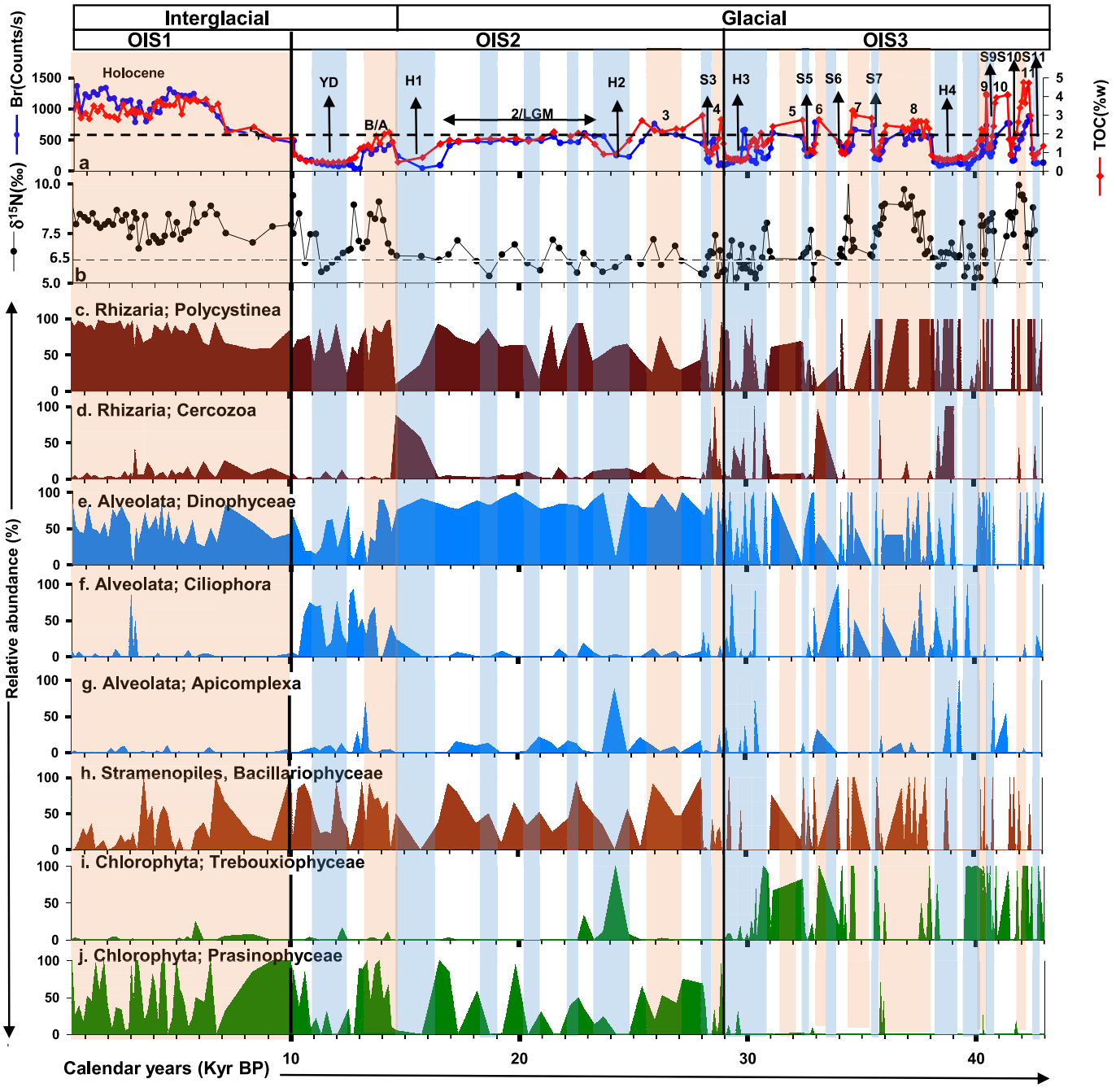

Fig. 2. Relative abundance of protist subgroups. (The same color coding and abbreviations as in Fig. 1.)

in OIS2 sediments (~20% of the total protist reads) and were generally below 5% of total protist reads during most of the Holocene (Fig. 1). However, diatoms showed cyclicity in abundance compared to other stramenopiles and represented up to 100% of stramenopile reads during interstadials of OIS3 as well as OIS2 and the early Holocene, while their relative abundance dropped during all stadials in OIS2 and OIS3 and at ~8.2 ka BP (Fig. 2). At the genus level, the primarily marine *Thalassiosira* was the most prominent diatom throughout the core, while coastal *Skeletonema* was the only diatom present during S11 and represented up to 80% of diatom reads during S3 (Fig. 3).

Green algae (Chlorophyta) identified in the Arabian Sea sediments comprised the unicellular pelagic families Trebouxiophyceae (exclusively the genus *Chlorella* in our record), Prasinophyceae, Chlorophyceae and Mamiellophyceae. Chlorophyta reads dominated the OIS3 reaching up to 50% of total protists with a notable exception of their general absence during long periods of strong denitrification and OMZ conditions such as during IS8 (Fig. 1). *Chlorella* dominated the green algal population during stadials of OIS3 and H2 when denitrification and OMZ conditions were reduced (Fig. 2). *Chlorella* was also dominant during IS5 when denitrification was less extensive compared to other interstadials (Fig. 2). Chlorophyte DNA was no longer abundant after H2 (Fig. 1), but a sharp shift in the relative abundance towards eutrophic Prasinophyceae as the most abundant chlorophytes was observed mainly during interstadials of OIS2 and the Holocene (Figs. 2 and 3).

Centroheliozoans (amoeboid protists) were sporadically abundant (up to 50%) in glacial OIS3 sediments and generally below the detection limit in OIS2 and OIS1 (Fig. 1). Reads of Haptophyte

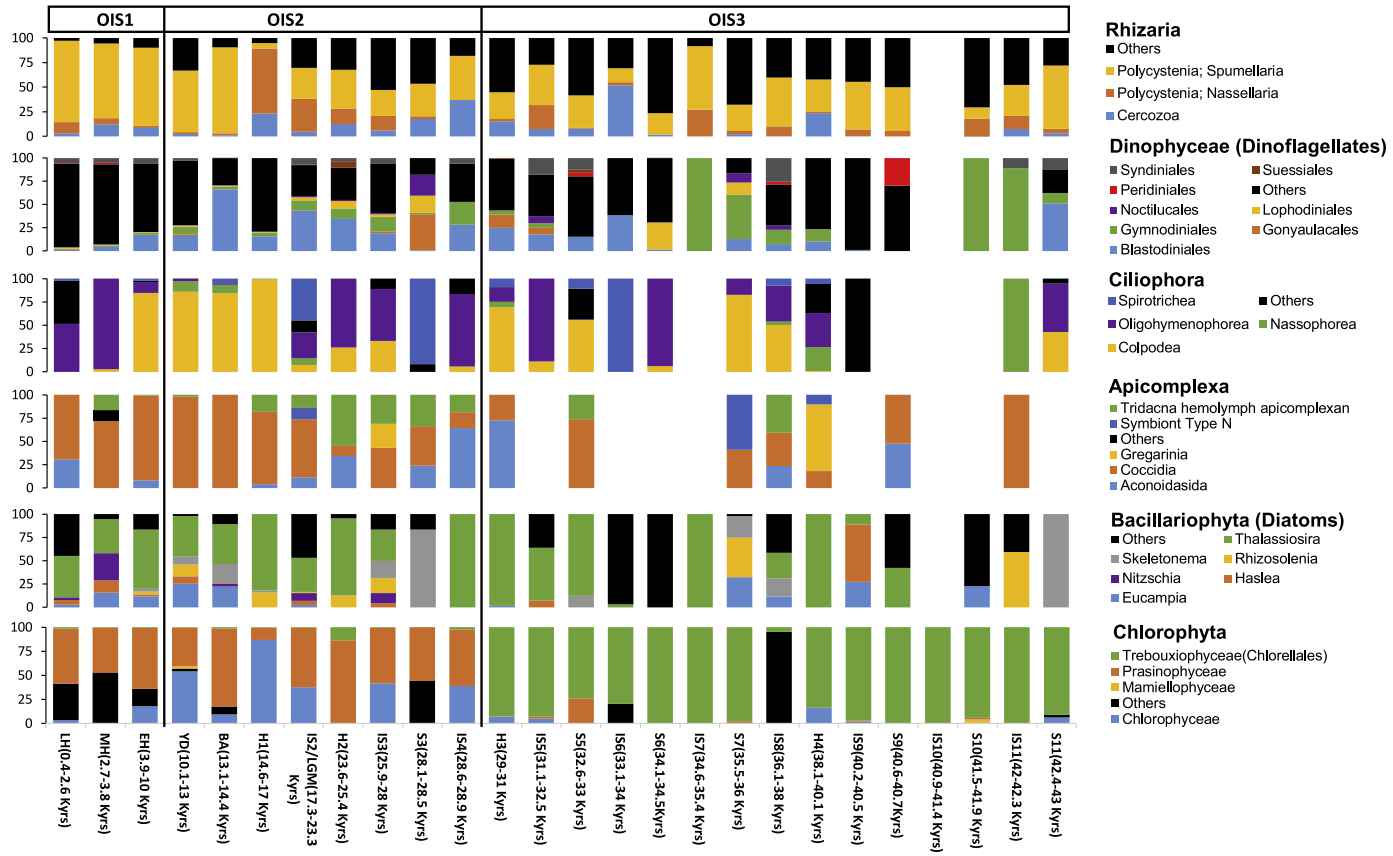

Fig. 3. Detailed protist abundance overview. Averaged relative abundance of essential sub-groups within the most abundant supergroups in different climate intervals are represented in stacked histograms. The time span of each grouped climate stage is denoted below the figure. Abbreviations: OIS (Oxygen Isotope Stage), LH (Late Holocene), MH (Mid Holocene), EH (Early Holocene), YD (Younger Dryas), B/A (Bølling-Allerød), H (Heinrich event), IS (Interstadial), S (Stadial).

algae were sporadically present throughout the core and comprised less than 5% of the reads notably during stadials such as H2 (Fig. 1). Other protist groups (Amoebozoa, Apuszoa, Choanoflagellida, Cryptophyta, Euglenozoa, Jakobida and Rhodophyta) (Fig. 1) were occasionally present and when combined, comprised less than 5% of the total protist sequences. In the analysis below, we focus exclusively on the most abundant protist groups that were frequently present and which contributed more than 5% to the total protist reads.

3.3. Correlation between change in paleoenvironment and protist community structure

To investigate the effect of OMZ strength on protist community compositions, we performed non metric multidimensional scaling analysis (NMDS; stress <0.05). Analysis of similarity (ANOSIM) revealed that the microbial communities were significantly different ($P = 0.001$) in sediments of the three categories described above (Fig. 4). In order to investigate which taxa were affected by strong vs. weak OMZ conditions and transitions we performed indicator species analysis (ISA).

3.4. Indicator species analysis

ISA identified 52 significant ($p < 0.05$) indicator taxa for category 1. Fig. S1 shows the specificity (A-value) vs. sensitivity (B-value) of each indicator species. In theory, an A-value of 1 indicates that the species in question occurs in only one indicator group, while an optimal B-value of 1 means that this species occurs in all samples of that category. Alveolata with 24 OTUs were the most abundant group of indicator species for Category 1. The

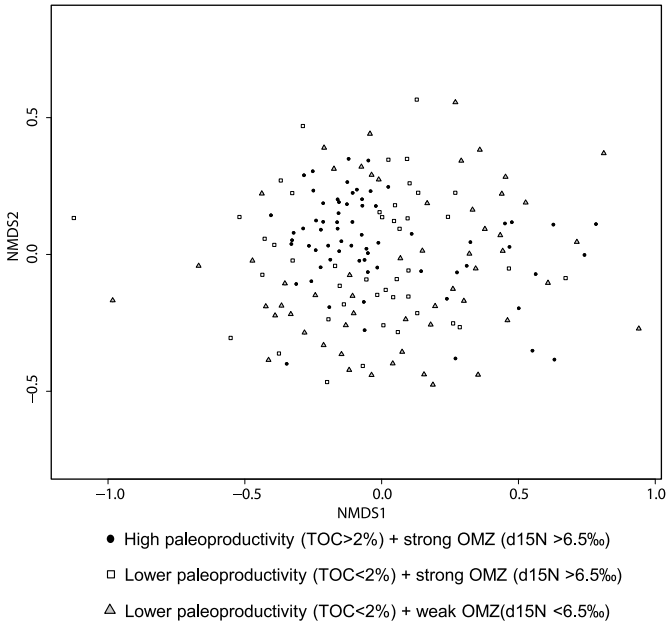

Fig. 4. NMDS analysis of community composition using all protist OTUs (stress <0.05). Analysis of similarity (ANOSIM) revealed that the overall protist community composition differed significantly between the three categories ($P = 0.001$). Axes in NMDS are arbitrary.

majority of these indicator species were dinoflagellates (13 OTUs), followed by unnamed alveolata (4 OTUs), marine alveolate group 1 (5 OTUs), and parasitic ciliates (Scuticoliliates, 2 OTUs). Syndiniales were among the most closely related dinoflagellates, whereas the

majority of the indicator dinoflagellates were related to environmental clones. Interestingly, two of the unclassified dinoflagellates (OTUs 52191 and 93979) showed 99% sequence similarity to clones isolated from anoxic waters of respectively Cariaco Basin (Genbank accession number GU820545.1) (Edgcomb et al., 2011), and the east Pacific rise (KJ761327) (Lie et al., 2014). The next important group indicative of this category were Rhizarians (i.e., cercozoans and polycystines). Indicator cercozoans belonged to Cercomonadida (2 OTUs: 11339 and 38346), Thecofilosea (4 OTUs) Silicofilosea (1 OTU) and un-named cercozoans (2OTUs: Cercozoa 1 and Cercozoa 2). Polycystinea contained 2 nassellarian members and spumellarian families Actinommidae (1 OTU), Ethmosphaeridae (1 OTU), Sphaerozoidae (3 OTUs) and Spongodiscidae (1 OTU). Chlorophytes (Prasinophytes) with 4 OTUs were also important indicators for category 1 along with unnamed Stramenopiles and one Oomycete OTU.

Thirty-two indicator species (16 Rhizaria, 12 Alveolata, and 4 Stramenopiles) were identified for category 2. Rhizarians belonging to the same polycystine families were found to be indicative of both categories 1 and 2. These involve spumellarian families Sphaerozoidae (3 OTUs), Actinommidae (1 OTU) and Ethmosphaeridae (1 OTU) plus 1 OTU of the nassellarian family Theoperidae. However, members of these families showed a generally stronger significance for category 1 (Fig. S1). Cercozoans, which were indicative of strong OMZ conditions and higher productivity were not indicative of less productive conditions during category 2.

Fewer and different dinoflagellates were found to be indicator species for category 2 (e.g. Blastodiniales) than for category 1. Category 2 also differed in the composition of indicator ciliates as it contained 4 OTUs of ciliates belonging to the class colpodea as opposed to scuticociliates indicative of category 1. Furthermore, apicomplexan parasites were indicators of category 2 as well as diatoms (Stramenopiles).

Only four important indicator species were identified for category 3 “weak OMZ conditions”: Chlorophyta (*Chlorella*), Centroheliozoa, and Rhizaria (Silicofilosea and an unnamed rhizarian) (Fig. S1).

4. Discussion

4.1. Interplay between past OMZ conditions and phototrophic protists

In agreement with modern observations of plankton-OMZ interactions in the NE Arabian Sea (Parab et al., 2006), our paleogenomics record also revealed an increase in the relative abundance of diatoms and mixotrophic dinoflagellates during glacial interstadials when SW monsoon and OMZ conditions were strong. In contrast, we observed a sharp decline in the relative abundance of diatom reads during stadials including Heinrich events when SW monsoon was weak (Deplazes et al., 2014). Our data further showed a decline in the relative abundance of diatoms and a predominance of dinoflagellates during the mid to late Holocene, which is likely due to deepening of anoxia as this was reported to result in dinoflagellates replacing diatoms in the modern-day NE Arabian Sea (Parab et al., 2006). Indeed, the Diatom/Dinoflagellate ratio (Dia/Dino index) is being used as a proxy to assess the environmental status of oceans (e.g. Wasmund et al., 2017). When nutrients get depleted, rapid sinking of diatom blooms reduces the food stock for zooplankton (i.e., a high Dia/Dino Index), but avails food to zoobenthos. A high Dia/Dino index is typically considered an indicator of good environmental status. In contrast, a low Dia/Dino index is indicative of eutrophication since dinoflagellate blooms support pelagic components of the food web (e.g. Wasmund et al., 2017). Therefore, the lowering of the Dia/Dino index suggests an increase in eutrophication and stratified anoxic conditions during the late Holocene in the NE Arabian Sea. Similar long-term trends in eutrophication and a resulting lower Dia/Dino index may alter the higher trophic levels of the marine food web in the context of predicted expansion of costal OMZs associated with global climate change.

Our data further revealed that *Chlorella* (Trebouxiophyceae) was an indicator species for weak OMZ conditions. *Chlorella* was relatively abundant in interstadial IS5, but otherwise predominated during the frequently occurring stadials of OIS3 and the H2 event in OIS2 (Fig. 2) when SW monsoon was weak and surface waters were likely to be depleted in key nutrients like nitrates (Deplazes et al., 2014). This abundance of *Chlorella* can be explained by the fact that under nitrogen stress *Chlorella* can survive by accumulation of fatty acids and carbohydrates in the cell membrane (Fan et al., 2014; Paes et al., 2016). Interestingly, Centroheliozoans also occurred during this period and were found to be a significant indicator species for weak OMZ conditions. Centroheliozoans as mentioned earlier are predatory amoeboid protists (Plotnikov and Ermolenko, 2015). However, they are also known to harbor endosymbiotic green algae such as *Chlorella* (Bubeck and Pfitzner, 2005), which would explain the co-occurrence of centroheliozoan reads with *Chlorella* in OIS3, and that both taxa were identified as significant indicator species for weak OMZs. Both *Chlorella* and Centroheliozoans were at or below detection limit during IS8 when according to the enriched δ^{15}N values, maximum denitrification and OMZ strength occurred, and when diatoms were the predominant primary producers instead (Fig. 2).

Chlorophytes as a group were no longer abundant protists after the OIS3–OIS2 transition, but *Chlorella* was succeeded by prasinophytes, which became the most abundant chlorophytes during the LGM and the Holocene (Figs. 1 and 2). Fossil pigments of prasinophytes generally serve as a proxy for past stratified dysoxic to anoxic waters (Roncaglia and Kuijpers, 2006). In our sedimentary 18S rDNA survey, prasinophytes were identified as important indicator taxa of strong OMZ with higher surface productivity. Deep mixing of nutrient-rich subsurface waters during SW monsoon brings nitrate into NE Arabian Sea surface waters (Madhupratap et al., 1996), which is required for the proliferation of prasinophytes (Prauss, 2007). Strengthening of the SW monsoon throughout and after the LGM (Schulz et al., 2002; von Rad et al., 1999) may have triggered the increased relative abundance of prasinophytes. In addition, elevated glacial sea surface salinity may have hindered prasinophytes from flourishing as they generally prefer brackish waters. Increased fluvial input from the Indus River, resulting into a reduced salinity after the LGM (Deplazes et al., 2014), may also have contributed to the growth of prasinophytes. Prasinophytes were absent or low in relative abundance during the cold stadials and the 8.2 ka event when weak monsoons resulted in reduced mixing (Singh et al., 2011; von Rad et al., 1995) and a scarcity of nutrients including nitrate must have prevailed. *Chlorella*, as a potential indicator for nutrient-limited conditions did not return as an abundant chlorophyte during the H1 and YD stadials. These events also experienced the continuous presence of dinoflagellates which are significant indicators of strong OMZ conditions, which suggests that OMZ conditions were not entirely absent during these events.

4.2. Interplay between past OMZ conditions and non-phototrophic protists

According to our paleogenomics survey, Alveolata (i.e., mixotrophic dinoflagellates, ciliates, and apicomplexans) represented a predominant group of protists during strong OMZ conditions (Figs. 1, 2 and 3). This is in agreement with current observations showing that during strong SW monsoons, dinoflagellates replace diatom blooms once anoxia starts to develop (Parab et al., 2006). The most abundant dinoflagellates were represented by members of the orders Blastodiniales, Gymnodiniales, and Syn-

diniales (Fig. 3). Blastodiniales are strictly parasitic dinoflagellates of zooplanktons and fish, while Syndiniales are either endosymbionts or parasites. Gymnodiniales are the least known groups of marine phytoplankton, but have been reported from suboxic interfaces and are known to form cysts as an adaptive strategy to survive adverse conditions such as low dissolved oxygen concentrations (Morquecho and Lechuga-Deveze, 2003) They are known ecto-parasites of zooplanktons (Coats, 1999). These dinoflagellates likely competed with a relatively large abundance of unclassified dinoflagellates with unknown growth requirements, notably during the entire Holocene (Fig. 3). It has been shown that stronger OMZs mainly occurred during interstadials after OIS3 when SW Monsoon intensified (Deplazes et al., 2014; Schulz et al., 2002). Our sedimentary DNA record is in agreement with this scenario since dinoflagellates fluctuated greatly in abundance between frequently alternating periods of strong vs. weak OMZ conditions during OIS3, but they became more continuously abundant during OIS2 and the Holocene, which experienced relatively long stretches of interstadials with increased SW monsoon intensity. Similar results with increased accumulation of dinoflagellates cysts during warm events of increased paleo-productivity such as the Holocene, B/A event and D/O interstadials has been witnessed in the anoxic Santa-Barbara basin (Pospelova et al., 2006). The second most abundant alveolates during strong OMZs were ciliates of the class Colpodea. Colpodeans are mostly freshwater ciliates that form cysts as a result of environmental stress. We observed an increase in the relative abundance of Colpodea during the B/A when high fluvial input from the Indus river was recorded in sediment cores obtained nearby (Deplazes et al., 2014). The next abundant ciliates were scuticociliates belonging to Oligohymenophorea, which contains endoparasites. Scuticociliates are obligate anaerobes that live in stratified low oxygen and anoxic marine waters in symbioses with sulfate reducing bacteria and methanogenic archaea and therefore serve as a proxy for OMZ conditions (Fenchel and Finlay, 1994). According to ISA, obligate endoparasitic pathogenic and spore-forming Apicomplexa (alveolata) were also significant indicators of strong OMZ conditions.

In addition to alveolata, rhizarians mainly represented by polycistine radiolarians and cercozoans (Fig. S1), also dominated during periods of stronger OMZs. Cercozoans, which mostly represent heterotrophic protists, were abundant and significant indicator species for strong OMZ with high surface productivity, while polycystine radiolarians were significant indicators of strong OMZ irrespective of productivity. Polycystine radiolarians often form symbiotic relationships with mainly dinoflagellates, prymnesiophytes and prasinophytes (Steineck and Casey, 1990). In this case dinoflagellates are enclosed in a thin envelope of cytoplasm produced by the radiolarian host's rhizopodial system. This provides ammonium and carbon dioxide for the dinoflagellate symbionts, and in return the dinoflagellates provide their radiolarian host with a jelly-like layer that serves for protection and to capture prey (Steineck and Casey, 1990). A co-existence of polycystine radiolarians, dinoflagellates and prasinophytes during strong OMZ periods was indeed observed in our molecular record. Combined, these results show that OMZ conditions shaped the past protist community by creating isolated habitats for those capable of sustaining oxygen depletion either by adapting a parasitic life cycle or by establishing mutualistic connections with others or by cyst formation, which is in accordance with recent observations from other OMZ impacted sites (Jing et al., 2015).

Differences in genomic 18S rRNA gene copy numbers between eukaryotes (Hou and Lin, 2009), prevent the ability to provide absolute quantitative data on past plankton. In addition, environmental DNA is prone to degradation. Nevertheless, our results show that stratigraphic analysis of sedimentary protist DNA can provide a useful long-term record of ecosystem responses to OMZ conditions including non-fossilizing taxa that traditionally escape microscopic identification in micro-paleontological studies. It is predicted that OMZs will continue to expand world-wide as a result of global warming and eutrophication (Helm et al., 2011; Keeling et al., 2010). Notably, our results suggest that long-term increase in eutrophication and a decrease in the Dia/Dino index, as has been the case in the NE Arabian Sea during the late Holocene, will likely favor the pelagic component of the marine food web in the context of predicted worldwide expansion of coastal OMZs associated with global climate change. Similar studies undertaken at other key locations with a history of persistent OMZs could provide a comprehensive window into past marine ecosystem changes and feedback mechanisms on OMZ expansion. If integrated with observations from modern time series, similar paleogenomic datasets could help towards forming a more comprehensive understanding and improved predictions of long-term OMZ expansion on coastal ecosystem interactions.

Acknowledgements

This work was primarily supported by NSF MGG Grant #1357017 to MJLC, VG, and LG. Additional financial support was provided via a C-DEBI grant #OCE-0939564 to WDO. We also thank the Curtin Office for Research and Development (ORD) for funding a PhD stipend to K.D.M. This is C-DEBI contribution #358. Core collection was supported by NSF OCE Grant #0634731 to LG. We thank the co-chiefs Peter Clift and Tim Henstock as well as the scientific participants, captain and crew of the *R/V* Pelagia. We thank Dr. Cornelia Wuchter and Dr. Alisson Blyth for helpful discussions. Data has been deposited to SRA (Sequence Read Archive) NCBI under Bio project: PRJNA397489 (SRP148586). We thank Dr. Christopher Somes (GEOMAR Helmholtz Centre for Ocean Research) and two anonymous reviewers and Editor Prof. Derek Vance for their constructive feedback.

Author contributions

M.J.L.C, V.G., and L.G. initiated and designed the study. M.J.L.C. and K.G. developed ideas. L.H. extracted DNA and performed PCR reactions. K.D.M. performed further experiments. K.D.M. and M.J.L.C. developed analytical tools. K.D.M. and W.D.O. analyzed data. K.D.M. and M.J.L.C. wrote the paper. K.D.M., M.J.L.C., and W.D.O. participated in data interpretation and all authors provided editorial comments on the manuscript.

Additional information

Supplementary information is available in the online version of the paper. Correspondence and requests for materials should be addressed to K.D.M. or M.J.L.C.

Competing financial interests

The authors declare no competing financial interests.

Appendix A. Supplementary material

Supplementary material related to this article can be found online at https://doi.org/10.1016/j.epsl.2018.05.045.

References

Amaral-Zettler, L.A., McCliment, E.A., Ducklow, H.W., Huse, S.M., 2009. A method for studying protistan diversity using massively parallel sequencing of V9 hypervariable regions of small-subunit ribosomal RNA genes. PLoS ONE 4, 6372.

Andruleit, H.A., von Rad, U., Bruns, A., Ittekkot, V., 2000. Coccolithophore fluxes from sediment traps in the northeastern Arabian Sea off Pakistan. Mar. Micropaleontol. 38, 285–308.

Banakar, V.K., Mahesh, B.S., Burr, G., Chodankar, A.R., 2010. Climatology of the Eastern Arabian Sea during the last glacial cycle reconstructed from paired measurement of foraminiferal δ^{18}O and Mg/Ca. Quat. Res. 73, 535–540.

Blackford, J.C., Burkill, P.H., 2002. Planktonic community structure and carbon cycling in the Arabian Sea as a result of monsoonal forcing: the application of a generic model. J. Mar. Syst. 36, 239–267.
Bubeck, J.A., Pfitzner, A.J.P., 2005. Isolation and characterization of a new type of chlorovirus that infects an endosymbiotic Chlorella strain of the heliozoon Acanthocystis turfacea. J. Gen. Virol. 86, 2871–2877.
Burkill, P.H., Edwards, E.S., John, A.W.G., Sleigh, M.A., 1993. Microzooplankton and their herbivorous activity in the Northeastern Atlantic-Ocean. Deep-Sea Res., Part 2, Top. Stud. Oceanogr. 40, 479–493.
Caporaso, J.G., Kuczynski, J., Stombaugh, J., Bittinger, K., Bushman, F.D., Costello, E.K., Fierer, N., Pena, A.G., Goodrich, J.K., Gordon, J.I., Huttley, G.A., Kelley, S.T., Knights, D., Koenig, J.E., Ley, R.E., Lozupone, C.A., McDonald, D., Muegge, B.D., Pirrung, M., Reeder, J., Sevinsky, J.R., Tumbaugh, P.J., Walters, W.A., Widmann, J., Yatsunenko, T., Zaneveld, J., Knight, R., 2010. QIIME allows analysis of high-throughput community sequencing data. Nat. Methods 7, 335–336.
Caporaso, J.G., Lauber, C.L., Walters, W.A., Berg-Lyons, D., Huntley, J., Fierer, N., Owens, S.M., Betley, J., Fraser, L., Bauer, M., Gormley, N., Gilbert, J.A., Smith, G., Knight, R., 2012. Ultra-high-throughput microbial community analysis on the Illumina HiSeq and MiSeq platforms. ISME J. 6, 1621–1624.
Cavalier-Smith, T., 1991. Cell diversification in heterotrophic flagellates. In: Patterson, D.J., Larsen, J. (Eds.), The Biology of Free-Living Heterotrophic Flagellates. Oxford University Press, Oxford, pp. 113–131.
Cavalier-Smith, T., 2002. The phagotrophic origin of eukaryotes and phylogenetic classification of protozoa. Int. J. Syst. Evol. Microbiol. 52, 297–354.
Clarke, K.R., 1993. Non-parametric multivariate analyses of changes in community structure. Aust. J. Ecol. 18, 117–143.
Clift, P.D., Giosan, L., Carter, A., Garzanti, E., Galy, V., Tabrez, A.R., Pringle, M., Campbell, I.H., France-Lanord, C., Blusztajn, J., Allen, C., Alizai, A., Lückge, A., Danish, M., Rabbani, M.M., 2010. Monsoon control over erosion patterns in the western himalaya: possible feed-back into the tectonic evolution. Geol. Soc. (Lond.) Spec. Publ. 342, 185–218.
Coats, D.W., 1999. Parasitic life styles of marine dinoflagellates. J. Eukaryot. Microbiol. 46, 402–409.
Coolen, M.J.L., Orsi, W.D., Balkema, C., Quince, C., Harris, K., Sylva, S.P., Filipova-Marinova, M., Giosan, L., 2013. Evolution of the plankton paleome in the Black Sea from the Deglacial to Anthropocene. Proc. Natl. Acad. Sci. USA 110, 8609–8614.
Deplazes, G., Luckge, A., Stuut, J.B.W., Patzold, J., Kuhlmann, H., Husson, D., Fant, M., Haug, G.H., 2014. Weakening and strengthening of the Indian monsoon during Heinrich events and Dansgaard–Oeschger oscillations. Paleoceanography 29, 99–114.
Direito, S.O.L., Marees, A., Roling, W.F.M., 2012. Sensitive life detection strategies for low-biomass environments: optimizing extraction of nucleic acids adsorbing to terrestrial and Mars analogue minerals. FEMS Microbiol. Ecol. 81, 111–123.
Dufrene, M., Legendre, P., 1997. Species assemblages and indicator species: the need for a flexible asymmetrical approach. Ecol. Monogr. 67, 345–366.
Edgcomb, V., Orsi, W., Bunge, J., Jeon, S., Christen, R., Leslin, C., Holder, M., Taylor, G.T., Suarez, P., Varela, R., Epstein, S., 2011. Protistan microbial observatory in the Cariaco Basin, Caribbean. I. Pyrosequencing vs Sanger insights into species richness. ISME J. 5, 1344–1356.
Fan, J.H., Cui, Y.B., Wan, M.X., Wang, W.L., Li, Y.G., 2014. Lipid accumulation and biosynthesis genes response of the oleaginous Chlorella pyrenoidosa under three nutrition stressors. Biotechnol. Biofuels 7.
Fenchel, T., Finlay, B.J., 1994. The evolution of life without oxygen. Am. Sci. 82, 22–29.
Helm, K.P., Bindoff, N.L., Church, J.A., 2011. Observed decreases in oxygen content of the global ocean. Geophys. Res. Lett. 38, 23602.
Hou, Y.B., Lin, S.J., 2009. Distinct gene number-genome size relationships for eukaryotes and non-eukaryotes: gene content estimation for dinoflagellate genomes. PLoS ONE 4, 6978.
Inagaki, F., Okada, H., Tsapin, A.I., Nealson, K.H., 2005. Microbial survival – the paleome: a sedimentary genetic record of past microbial communities. Astrobiology 5, 141–153.
Jing, H., Rocke, E., Kong, L., Xia, X., Liu, H., Landry, M.R., 2015. Protist communities in a marine oxygen minimum zone off Costa Rica by 454 pyrosequencing. Biogeosci. Discuss. 2015, 13483–13509.
Keeling, R.F., Kortzinger, A., Gruber, N., 2010. Ocean deoxygenation in a warming world. Annu. Rev. Mar. Sci. 2, 199–229.
Kobashi, T., Severinghaus, J.P., Brook, E.J., Barnola, J.M., Grachev, A.M., 2007. Precise timing and characterization of abrupt climate change 8200 years ago from air trapped in polar ice. Quat. Sci. Rev. 26, 1212–1222.
Lejzerowicz, F., Esling, P., Majewski, W., Szczucinski, W., Decelle, J., Obadia, C., Arbizu, P.M., Pawlowski, J., 2013. Ancient DNA complements microfossil record in deep-sea subsurface sediments. Biol. Lett. 9, 0283.
Lie, A.A.Y., Liu, Z.F., Hu, S.K., Jones, A.C., Kim, D.Y., Countway, P.D., Amaral-Zettler, L.A., Cary, S.C., Sherr, E.B., Sherr, B.F., Gast, R.J., Caron, D.A., 2014. Investigating microbial eukaryotic diversity from a global census: insights from a comparison of pyrotag and full-length sequences of 18S rRNA genes. Appl. Environ. Microbiol. 80, 4363–4373.
Madhupratap, M., Kumar, S.P., Bhattathiri, P.M.A., Kumar, M.D., Raghukumar, S., Nair, K.K.C., Ramaiah, N., 1996. Mechanism of the biological response to winter cooling in the northeastern Arabian Sea. Nature 384, 549–552.
Morquecho, L., Lechuga-Deveze, C.H., 2003. Dinoflagellate cysts in recent sediments from Bahía Concepción Gulf of California. Bot. Mar. 46, 132–141.
Oksanen, J., 2011. Multivariate analysis of ecological communities in R: vegan tutorial. R package version 1.17-7 ed.
Orsi, W.D., Coolen, M.J.L., Wuchter, C., He, L., More, K.D., Irigoien, X., Chust, G., Johnson, C., Hemingway, J.D., Lee, M., Galy, V., Giosan, L., 2017. Climate oscillations reflected within the microbiome of Arabian Sea sediments. Sci. Rep. 7, 6040.
Paes, C.R.P.S., Faria, G.R., Tinoco, N.A.B., Castro, D.J.F.A., Barbarino, E., Lourenco, S.O., 2016. Growth, nutrient uptake and chemical composition of *Chlorella sp* and *Nannochloropsis oculata* under nitrogen starvation. Lat. Am. J. Aquat. Res. 44, 275–292.
Parab, S.G., Matondkar, S.G.P., Gomes, H.D., Goes, J.I., 2006. Monsoon driven changes in phytoplankton populations in the eastern Arabian Sea as revealed by microscopy and HPLC pigment analysis. Cont. Shelf Res. 26, 2538–2558.
Plotnikov, A.O., Ermolenko, E.A., 2015. Centrohelid heliozoa (Chromista, Hacrobia) of Southern Cis-Ural region. Biol. Bull. 42, 683–695.
Pospelova, V., Pedersen, T.F., de Vernal, A., 2006. Dinoflagellate cysts as indicators of climatic and oceanographic changes during the past 40 kyr in the Santa Barbara Basin, southern California. Paleoceanography 21, PA2010.
Prauss, M.L., 2007. Availability of reduced nitrogen chemospecies in photic-zone waters as the ultimate cause for fossil prasinophyte prosperity. Palaios 22, 489.
Pruesse, E., Quast, C., Knittel, K., Fuchs, B.M., Ludwig, W.G., Peplies, J., Glockner, F.O., 2007. SILVA: a comprehensive online resource for quality checked and aligned ribosomal RNA sequence data compatible with ARB. Nucleic Acids Res. 35, 7188–7196.
Roncaglia, L., Kuijpers, A., 2006. Revision of the palynofacies model of Tyson (1993) based on recent high-latitude sediments from the North Atlantic. Facies 52, 19–39.
Schulte, S., Muller, P.J., 2001. Variations of sea surface temperature and primary productivity during Heinrich and Dansgaard–Oeschger events in the northeastern Arabian Sea. Geo Mar. Lett. 21, 168–175.
Schulz, H., Rad, U., Erlenkeuser, H., 1998. Correlation between Arabian Sea and Greenland climate oscillations of the past 110,000 years. Nature 393, 54–57.
Schulz, H., von Rad, U., Ittekkot, V., 2002. Planktic foraminifera, particle flux and oceanic productivity off Pakistan, NE Arabian Sea: modern analogues and application to the palaeoclimatic record. Geol. Soc. (Lond.) Spec. Publ. 195, 499–516.
Schulz, H., Von Rad, U., Von Stackelberg, U., 1996. Laminated sediments from the oxygen-minimum zone of the Northeastern Arabian Sea. Geol. Soc. (Lond.) Spec. Publ. 116, 185–207.
Sherr, E.B., Sherr, B.F., 1994. Bacterivory and herbivory – key roles of phagotrophic protists in pelagic food webs. Microb. Ecol. 28, 223–235.
Singh, A.D., Jung, S.J.A., Darling, K., Ganeshram, R., Ivanochko, T., Kroon, D., 2011. Productivity collapses in the Arabian Sea during glacial cold phases. Paleoceanography 26, PA3210.
Steineck, P.L., Casey, R.E., 1990. Ecology and paleobiology of foraninifera and radiolaria. In: Capriulo, G.M. (Ed.), Ecology of Marine Protozoa. Oxford University Press, Oxford.
Strom, S.L., Welschmeyer, N.A., 1991. Pigment-specific rates of phytoplankton growth and microzooplankton grazing in the open sub-arctic Pacific ocean. Limnol. Oceanogr. 36, 50–63.
Stuiver, M., Reimer, P.J., 1993. Extended C-14 data-base and revised Calib 3.0 C-14 age calibration program. Radiocarbon 35, 215–230.
von Rad, U., Schulz, H., Khan, A.A., Ansari, M., Berner, U., Cepek, P., Cowie, G., Dietrich, P., Erlenkeuser, H., Geyh, M., Jennerjahn, T., Luckge, A., Marchig, V., Riech, V., Rosch, H., Schafer, P., Schulte, S., Sirocko, F., Tahir, M., Weiss, W., 1995. Sampling the oxygen minimum zone off Pakistan: glacial–interglacial variations of anoxia and productivity (preliminary-results, Sonne-90 cruise). Mar. Geol. 125, 7–19.
von Rad, U., Schulz, H., Riech, V., den Dulk, M., Berner, U., Sirocko, F., 1999. Multiple monsoon-controlled breakdown of oxygen-minimum conditions during the past 30,000 years documented in laminated sediments off Pakistan. Palaeogeogr. Palaeoclimatol. Palaeoecol. 152, 129–161.
Wasmund, N., Kownacka, J., Gobel, J., Jaanus, A., Johansen, M., Jurgensone, I., Lehtinen, S., Powilleit, M., 2017. The Diatom/Dinoflagellate index as an indicator of ecosystem changes in the Baltic Sea 1. Principle and handling instruction. Front. Mar. Sci. 4, 22.
Worden, A.Z., Follows, M.J., Giovannoni, S.J., Wilken, S., Zimmerman, A.E., Keeling, P.J., 2015. Rethinking the marine carbon cycle: factoring in the multifarious lifestyles of microbes. Science 347, 1257594.
Wright, J.J., Konwar, K.M., Hallam, S.J., 2012. Microbial ecology of expanding oxygen minimum zones. Nat. Rev. Microbiol. 10, 381–394.
Ziegler, M., Jilbert, T., de Lange, G.J., Lourens, L.J., Reichart, G.J., 2008. Bromine counts from XRF scanning as an estimate of the marine organic carbon content of sediment cores. Geochem. Geophys. Geosyst. 9, Q05009.